Spatial coherence measurement and partially coherent diffractive imaging using self-referencing holography

Shao, Yifeng; Lu, Xingyuan; Konijnenberg, Sander; Zhao, Chengliang; Cai, Yangjian; Urbach, Paul

DOI
10.1364/OE.26.004479

Publication date
2018

Document Version
Final published version

Published in
Optics Express

Research Article | Vol. 26, No. 4 | 19 Feb 2018 | OPTICS EXPRESS 4479
Optics EXPRESS

Spatial coherence measurement and partially coherent diffractive imaging using self-referencing holography

YIFENG SHAO,[1] XINGYUAN LU,[2,3] SANDER KONIJNENBERG,[1] CHENGLIANG ZHAO,[2,3,*] YANGJIAN CAI,[2,3] AND H. PAUL URBACH[1]

[1] *Optics Research Group, Imaging Physics Department, Delft University of Technology, The Netherlands*
[2] *College of Physics, Optoelectronics and Energy and Collaborative Innovation Center of Suzhou Nano Science and Technology, Soochow University, China*
[3] *Key Lab of Advanced Optical Manufacturing Technologies of Jiangsu Province and Key Lab of Modern Optical Technologies of Education Ministry of China, Soochow University, China*
[*] *zhaochengliang@suda.edu.cn*

Abstract: The complete characterization of spatial coherence is extremely difficult because the mutual coherence function (MCF) is a complex-valued function of four independent Cartesian coordinates. This difficulty limits the ability to control and to optimize the spatial coherence in a broad range of key applications. Here we propose an efficient and robust scheme for measuring the complete MCF of an arbitrary partially coherent beam using self-referencing holography, which does not require any prior knowledge or making any assumptions about the MCF. We further apply our method to lensless diffractive imaging, and experimentally demonstrate the reconstruction of a phase object under spatially partially coherent illumination. This application is particularly useful for imaging at short wavelengths, where the illumination sources lack spatial coherence and no high-quality imaging optics are available.

OCIS codes: (030.1640) Coherence; (090.1995) Digital holography; (110.1758) Computational imaging.

References and links

1. Y. Cai, Y. Chen, and F. Wang, "Generation and propagation of partially coherent beams with nonconventional correlation functions: a review [invited]," J. Opt. Soc. Am. A **31**, 2083–2096 (2014).
2. Y. Chen, F. Wang, L. Liu, C. Zhao, Y. Cai, and O. Korotkova, "Generation and propagation of a partially coherent vector beam with special correlation functions," Phys. Rev. A **89**, 013801 (2014).
3. G. Gbur, "Partially coherent beam propagation in atmospheric turbulence [invited]," J. Opt. Soc. Am. A **31**, 2038–2045 (2014).
4. K. Lai, A. E. Rosenbluth, S. Bagheri, J. Hoffnagle, K. Tian, D. Melville, J. Tirapu-Azpiroz, M. Fakhry, Y. Kim, S. Halle, G. McIntyre, A. Wagner, G. Burr, M. Burkhardt, D. Corliss, E. Gallagher, T. Faure, M. Hibbs, D. Flagello, J. Zimmermann, B. Kneer, F. Rohmund, F. Hartung, C. Hennerkes, M. Maul, R. Kazinczi, A. Engelen, R. Carpaij, R. Groenendijk, J. Hageman, and C. Russ, "Experimental result and simulation analysis for the use of pixelated illumination from source mask optimization for 22nm logic lithography process," in "SPIE Advanced Lithography,"vol. 7274 (International Society for Optics and Photonics, 2009), p. 72740.
5. K. M. Douglass, C. Sieben, A. Archetti, A. Lambert, and S. Manley, "Super-resolution imaging of multiple cells by optimized flat-field epi-illumination," Nat. Photon. **10**, 705–708 (2016).
6. H. Partanen, J. Turunen, and J. Tervo, "Coherence measurement with digital micromirror device," Opt. Lett. **39**, 1034–1037 (2014).
7. F. Pfeiffer, O. Bunk, C. Schulze-Briese, A. Diaz, T. Weitkamp, C. David, J. F. van der Veen, I. Vartanyants, and I. K. Robinson, "Shearing interferometer for quantifying the coherence of hard X-ray beams," Phys. Rev. Lett. **94**, 164801 (2005).
8. S. Divitt and L. Novotny, "Spatial coherence of sunlight and its implications for light management in photovoltaics," Optica **2**, 95–103 (2015).
9. D. Morrill, D. Li, and D. Pacifici, "Measuring subwavelength spatial coherence with plasmonic interferometry," Nat. Photon. **10**, 681–687 (2016).
10. S. Marathe, X. Shi, M. J. Wojcik, N. G. Kujala, R. Divan, D. C. Mancini, A. T. Macrander, and L. Assoufid, "Probing transverse coherence of X-ray beam with 2D phase grating interferometer," Opt. Express **22**, 14041–14053 (2014).
11. X. Shi, S. Marathe, M. J. Wojcik, N. G. Kujala, A. T. Macrander, and L. Assoufid, "Circular grating interferometer for mapping transverse coherence area of X-ray beams," Appl. Phys. Lett. **105**, 041116 (2014).

#314717 https://doi.org/10.1364/OE.26.004479
Journal © 2018 Received 30 Nov 2017; revised 7 Feb 2018; accepted 7 Feb 2018; published 12 Feb 2018

Optics EXPRESS

12. X. Liu, F. Wang, L. Liu, Y. Chen, Y. Cai, and S. A. Ponomarenko, "Complex degree of coherence measurement for classical statistical fields," Opt. Lett. **42**, 77–80 (2017).
13. C. Q. Tran, G. J. Williams, A. Roberts, S. Flewett, A. G. Peele, D. Paterson, M. D. de Jonge, and K. A. Nugent, "Experimental measurement of the four-dimensional coherence function for an undulator X-ray source," Phys. Rev. Lett. **98**, 224801 (2007).
14. L. Waller, G. Situ, and J. W. Fleischer, "Phase-space measurement and coherence synthesis of optical beams," Nat. Photon. **6**, 474–479 (2012).
15. J. K. Wood, K. A. Sharma, S. Cho, T. G. Brown, and M. A. Alonso, "Using shadows to measure spatial coherence," Opt. Lett. **39**, 4927–4930 (2014).
16. K. A. Sharma, T. G. Brown, and M. A. Alonso, "Phase-space approach to lensless measurements of optical field correlations," Opt. Express **24**, 16099–16110 (2016).
17. J. N. Clark, X. Huang, R. Harder, and I. K. Robinson, "High-resolution three-dimensional partially coherent diffraction imaging," Nat. Commun. **3**, 993 (2012).
18. N. Burdet, X. Shi, D. Parks, J. N. Clark, X. Huang, S. D. Kevan, and I. K. Robinson, "Evaluation of partial coherence correction in X-ray ptychography," Opt. Express **23**, 5452–5467 (2015).
19. L. W. Whitehead, G. J. Williams, H. M. Quiney, D. J. Vine, R. A. Dilanian, S. Flewett, K. A. Nugent, A. G. Peele, E. Balaur, and I. McNulty, "Diffractive imaging using partially coherent X rays," Phys. Rev. Lett. **103**, 243902 (2009).
20. P. Thibault and A. Menzel, "Reconstructing state mixtures from diffraction measurements," Nature. **494**, 68–71 (2013).
21. I. McNulty, J. Kirz, C. Jacobsen, E. H. Anderson, M. R. Howells, and D. P. Kern, "High-resolution imaging by Fourier transform X-ray holography," Science **256**, 1009 (1992).
22. S. Eisebitt, J. Lüning, W. Schlotter, M. Lörgen, O. Hellwig, W. Eberhardt, and J. Stöhr, "Lensless imaging of magnetic nanostructures by X-ray spectro-holography," Nature. **432**, 885–888 (2004).
23. L.-M. Stadler, C. Gutt, T. Autenrieth, O. Leupold, S. Rehbein, Y. Chushkin, and G. Grübel, "Hard X-ray holographic diffraction imaging," Phys. review letters **100**, 245503 (2008).
24. J. L. Codona, "Differential optical transfer function wavefront sensing," Opt. Eng. **52**, 097105 (2013).
25. S. Lai, B. King, and M. A. Neifeld, "Wave front reconstruction by means of phase-shifting digital in-line holography," Opt. Commun. **173**, 155–160 (2000).
26. A. Konijnenberg, W. Coene, and H. Urbach, "Non-iterative phase retrieval by phase modulation through a single parameter," Ultramicroscopy **174**, 70–78 (2017).
27. P. Gao, B. Yao, I. Harder, N. Lindlein, and F. J. Torcal-Milla, "Phase-shifting Zernike phase contrast microscopy for quantitative phase measurement," Opt. letters **36**, 4305–4307 (2011).
28. A. Maiden, G. Morrison, B. Kaulich, A. Gianoncelli, and J. Rodenburg, "Soft X-ray spectromicroscopy using ptychography with randomly phased illumination," Nat. Commun. **4**, 1669 (2013).

1. Introduction

Spatial coherence is among the fundamental properties of light. It describes the statistical correlation between fields at a pair of locations. However, the measurement of spatial coherence is remarkably challenging, which limits the control and the optimization of spatial coherence in a broad range of key applications such as beam shaping [1, 2], optical communication through a turbulent atmosphere [3], illumination for advanced imaging systems (e.g. optical lithography) [4] and superresolution imaging [5]. The spatial coherence of a beam is described by the complex-valued 4-dimensional mutual coherence function (MCF). The process of measuring the MCF is time consuming, especially for methods measuring the intensity-intensity correlation [1, 2] or the interference pattern [6] at all pairs of locations. Other interference based methods measure the fringe visibility in a single direction [7–9] or multiple directions [10, 11]. These methods rely on the symmetric structure of the MCF, and the method reported recently in [12] on an analytic model of the MCF, e.g the Gaussian Schell-model. Spatial coherence can alternatively be determined using the so-called phase space methods [13–16]. However, the phase space methods, as well as other proposed methods in [1, 2, 10, 11], cannot measure both the amplitude and the phase of the MCF. The phase of the MCF has direct impact on the propagation of a partially coherent beam and is of importance for other phase-sensitive applications.

In diffractive imaging, it is essential to characterize the spatial coherence. The aim of diffractive imaging is to reconstruct the transmission or reflection function of an object from the diffracted far-field intensity. In the X-ray and electron regime, diffractive imaging is particularly useful for imaging nanoscale structures. However, the lack of spatial coherence of the illumination sources

Optics EXPRESS

severely degrades the performance of imaging. Experimentally, an almost completely coherent beam can only be obtained by using coherence filtering but this comes at the price of losing a significant amount of beam flux.

In order to utilize the partially coherent beam for illumination, widely used iterative algorithms have been modified to take into account the propagation of the MCF instead of the coherent electromagnetic field. In [17, 18], the authors interpret the recorded intensity as a convolution between the coherent diffraction pattern and a shift-invariant MCF. Other methods are based on the mode decomposition of the MCF [19, 20]. However, these modifications are effective only for beams whose degree of spatial coherence are rather high. Meanwhile, to our knowledge, none of the non-iterative algorithms, e.g. [21–23], have been adapted to utilize partially coherent beams, despite the benefit of instant and unambiguous reconstruction of the object.

In this paper, we present a method for measuring the complete MCF of an arbitrary spatially partially coherent light beam. Our method does not require any prior knowledge, or make any assumptions about the MCF of the spatially partially coherent beam. In our method, the beam propagate through an aperture and we measure the intensities of the diffraction pattern in the far-field. We perturb the transmission function of the aperture plane at a particular point, where we either use a phase plate to change the phase of the light (when the perturbation is inside the aperture) or introduce a pinhole that lets light propagate through (when the perturbation is outside the aperture). A 2-dimensional function that describes the correlation between the fields at the perturbation point and at all other locations can be retrieved from the measurements of the far-field intensities using holography. Therefore, the complete 4-dimensional MCF can be obtained by scanning the location of the perturbation point in the 2-dimensional aperture plane.

Our method can be turned into a non-iterative diffractive imaging method by superposing the aperture with a transmissive object. In this situation, we retrieve the product of the object's transmission function and the correlation function of the incident beam with respect to the perturbation point, which plays a role as the modulation. After having calibrated and compensated for the modulation, we obtain the object's transmission function alone. The modulation also influences the requirement of signal-to-noise ratio of the diffractive imaging.

Here we investigate the performance of our method using beams of various types of correlation structures for different degrees of coherence via a proof-of-principle experiment at visible wavelength. Because we use a lensless configuration, by scaling the size of the aperture and the perturbation point, our method be used at any wavelength.

2. Principle of spatial coherence measurement and diffractive imaging using spatially partially coherent illmination

The spatial coherence properties of a beam have direct influence on its far-field intensity distribution. We can describe a spatially partially coherent beam by its MCF, which gives the correlation between fields at a pair of points. If the fields at two points are completely uncorrelated, their far-field intensities will added up incoherently and no interference occurs, while in other cases, the fields at the two points are partially correlated with each other, and the contrast of the fringe visibility of their interference pattern is associated with the degree of spatial coherence. This effect is illustrated in Fig 1, where we let a partially coherent beam propagate through an aperture and then through a transmissive object, and the far-field diffraction pattern is observed. As the illumination becomes less coherent, the diffraction pattern becomes more blurred. This blur degrades the performance of diffractive imaging, but it also carries valuable information of the illumination beam which can be retrieved for characterising the spatial coherence properties. Conversely, the knowledge of the spatial coherence properties will help to reconstruct the object even though it is illuminated by spatially partially coherent light.

We generate the spatially partially coherent using an extended planar incoherent source. In the source plane, the light is spatially incoherent, however, after propagating to the plane where

Optics EXPRESS

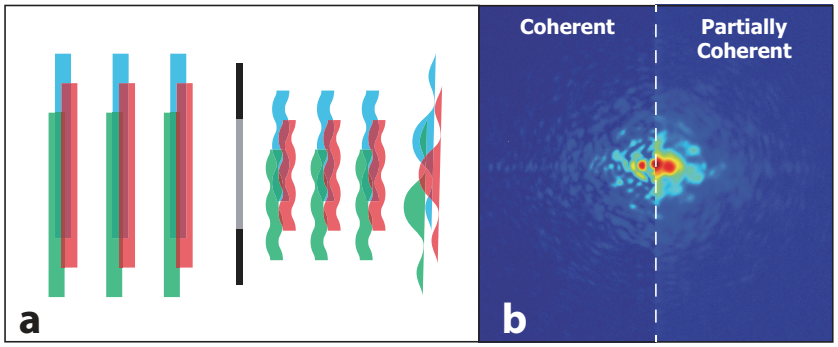

Fig. 1. The influence of spatial partial coherence on the propagation of light field and the diffractive imaging (experiment results). (a): Schematic plot of the experimental setup. We let a partially coherent beam propagate through an aperture which is superposed with a transmissive object, and observe the far-field diffracted intensity distribution. (b): The comparison between the intensity measurements of the coherent beam and the partially coherent beam. The blur of the diffraction pattern carries information about the spatial coherence properties of the beam.

we place the aperture, the light becomes spatially partially coherent. We denote the MCF of the light at the aperture plane by $J(\mathbf{r}_1, \mathbf{r}_2)$, where $(\mathbf{r}_1, \mathbf{r}_2)$ represent the locations of two points in the aperture plane. $J(\mathbf{r}_1, \mathbf{r}_2)$ describes the correlation between the fields at these two points, and is determined by the intensity distribution of the source.

In the experimental setup shown by Fig 1, we superpose a transmissive object with the aperture, so the transmission function of the aperture plane is given by $T(\mathbf{r}) = P(\mathbf{r})O(\mathbf{r})$, where $P(\mathbf{r})$ and $O(\mathbf{r})$ are the transmission function of the aperture and the transmissive object respectively. The value of $P(\mathbf{r})$ is one inside the aperture and zero outside the aperture, while $O(\mathbf{r})$ is a complex-valued function. After propagating through the aperture and the transmissive object superposed with the aperture, the diffraction pattern generated by the partially coherent beam can be observed in the far-field, which can be expressed by:

$$I_0(\mathbf{k}) = \iiiint T(\mathbf{r}_1)T(\mathbf{r}_2)^* J(\mathbf{r}_1, \mathbf{r}_2) \exp[-i2\pi\mathbf{k} \cdot (\mathbf{r}_1 - \mathbf{r}_2)] \mathrm{d}^2\mathbf{r}_1 \mathrm{d}^2\mathbf{r}_2, \tag{1}$$

where $\mathbf{k}$ denotes the coordinate of the measurement plane. Here we neglect the dependence of the object's transmission function on the incident angle of the illuminating wave, and the vignetting effect casued by the aperture.

In Eq. (1), the MCF $J(\mathbf{r}_1, \mathbf{r}_2)$ is a 4-dimensional complex-valued function. Each of the two points $(\mathbf{r}_1, \mathbf{r}_2)$ requires two independent coordinates to identify the location in the aperture plane, so in total four independent coordinates are required. Thus, Eq. (1) contains a four-fold integral, and the computation of the diffraction pattern using Eq. (1) is so time-consuming that neither the MCF of the illumination beam $J(\mathbf{r}_1, \mathbf{r}_2)$ nor the transmission function $T(\mathbf{r})$ of the aperture plane can be retrieved from the intensity measurements of the diffraction pattern

In our method, we introduce a localized point perturbation to the transmission function of the aperture plane. Our method is similar to holographic methods [21–26] in the sense that we measure the patterns due to the interference between the field at the location of the perturbation point (the reference wave) and the field propagating through the aperture and the transmissive object (the object wave). It is called "self-referencing holography" because the reference wave is part of the object wave. This guarantees that the reference wave is correlated with the object wave, so that interference can take place.

Optics EXPRESS

2.1. Retrieving the MCF and the object using self-referencing holography

We approximate the region of perturbation by a delta function $\delta(\mathbf{r}-\mathbf{r}_0)$, where $\mathbf{r}_0$ denotes the location of the perturbation point. In general, the perturbed transmission function can be written as

$$T'(\mathbf{r}) = T(\mathbf{r}) + \gamma\delta(\mathbf{r}-\mathbf{r}_0). \tag{2}$$

If the perturbation corresponds to a pinhole introduced at a point $\mathbf{r}_0$ that is located outside the aperture (i.e. $T(\mathbf{r}_0)=0$) see Fig. 2(b) and 2(c), then the term $\gamma\delta(\mathbf{r}-\mathbf{r}_0)$ introduces extra energy contribution that breaks the energy conservation. If the perturbation corresponds to a phase change ϕ of the light at a point $\mathbf{r}_0$ that is located out side the aperture (i.e. $T(\mathbf{r}_0)\neq 0$) see Fig. 2.(a), then $\gamma = [\exp(i\phi)-1]T(\mathbf{r}_0)$, so that $T'(\mathbf{r}_0) = T(\mathbf{r}_0)\exp(i\phi)$ and the energy is conserved.

By substituting $T'(\mathbf{r})$ into Eq. (1) to replace $T(\mathbf{r})$, we obtain the expression for the perturbed diffraction pattern as follows:

$$\begin{aligned} I(\mathbf{k}) = \iiiint & [T(\mathbf{r}_1)+\gamma\delta(\mathbf{r}_1-\mathbf{r}_0)][T(\mathbf{r}_2)+\gamma\delta(\mathbf{r}_2-\mathbf{r}_0)]^* \\ & \times J(\mathbf{r}_1,\mathbf{r}_2)\exp[-i2\pi\mathbf{k}\cdot(\mathbf{r}_1-\mathbf{r}_2)]\mathrm{d}^2\mathbf{r}_1\mathrm{d}^2\mathbf{r}_2. \end{aligned} \tag{3}$$

Expanding the brackets in this expression leads to four terms:

$$\begin{aligned} I(\mathbf{k}) = & \iiiint T(\mathbf{r}_1)T(\mathbf{r}_2)^*J(\mathbf{r}_1,\mathbf{r}_2)\exp[-i2\pi\mathbf{k}\cdot(\mathbf{r}_1-\mathbf{r}_2)]\mathrm{d}^2\mathbf{r}_1\mathrm{d}^2\mathbf{r}_2 \\ & + \iiiint [\gamma\delta(\mathbf{r}_1-\mathbf{r}_0)][\gamma\delta(\mathbf{r}_2-\mathbf{r}_0)]^* \\ & \quad \times J(\mathbf{r}_1,\mathbf{r}_2)\exp[-i2\pi\mathbf{k}\cdot(\mathbf{r}_1-\mathbf{r}_2)]\mathrm{d}^2\mathbf{r}_1\mathrm{d}^2\mathbf{r}_2 \\ & + \iiiint [\gamma\delta(\mathbf{r}_2-\mathbf{r}_0)]^*T(\mathbf{r}_1)J(\mathbf{r}_1,\mathbf{r}_2)\exp[-i2\pi\mathbf{k}\cdot(\mathbf{r}_1-\mathbf{r}_2)]\mathrm{d}^2\mathbf{r}_1\mathrm{d}^2\mathbf{r}_2 \\ & + \iiiint [\gamma\delta(\mathbf{r}_1-\mathbf{r}_0)]T(\mathbf{r}_2)^*J(\mathbf{r}_1,\mathbf{r}_2)\exp[-i2\pi\mathbf{k}\cdot(\mathbf{r}_1-\mathbf{r}_2)]\mathrm{d}^2\mathbf{r}_1\mathrm{d}^2\mathbf{r}_2 \\ & = I_0(\mathbf{k}) + |(\gamma-1)T(\mathbf{r}_0)|^2J(\mathbf{r}_0,\mathbf{r}_0) \\ & + \iint \gamma^*T(\mathbf{r}_1)J(\mathbf{r}_1,\mathbf{r}_0)\exp[-i2\pi\mathbf{k}\cdot(\mathbf{r}_1-\mathbf{r}_0)]\mathrm{d}^2\mathbf{r}_1 \\ & + \iint \gamma T(\mathbf{r}_2)^*J(\mathbf{r}_0,\mathbf{r}_2)\exp[-i2\pi\mathbf{k}\cdot(\mathbf{r}_0-\mathbf{r}_2)]\mathrm{d}^2\mathbf{r}_2, \end{aligned} \tag{4}$$

where the first term is the original diffraction pattern $I_0(\mathbf{k})$ given by Eq. (1), the second term is a constant term, and the last two terms are referred to as the "interference terms". Now we substitute the integration variables of the two interference terms by

$$\begin{cases} \mathbf{r} = \mathbf{r}_1 - \mathbf{r}_0 \\ \mathbf{r} = \mathbf{r}_0 - \mathbf{r}_2 \end{cases} \Longrightarrow \begin{cases} \mathbf{r}_1 = \mathbf{r}_0 + \mathbf{r} \\ \mathbf{r}_2 = \mathbf{r}_0 - \mathbf{r} \end{cases}, \tag{5}$$

and we use Hermitian property of the MCF in the two interference term. Finally we obtain that

$$\begin{aligned} I(\mathbf{k}) = & I_0(\mathbf{k}) + |\gamma|^2J(\mathbf{r}_0,\mathbf{r}_0) \\ & + \iint \gamma^*[T(\mathbf{r}_0+\mathbf{r})J(\mathbf{r}_0+\mathbf{r},\mathbf{r}_0)]\exp[-i2\pi\mathbf{k}\cdot\mathbf{r}]\mathrm{d}^2\mathbf{r} \\ & + \iint \gamma[T(\mathbf{r}_0-\mathbf{r})J(\mathbf{r}_0-\mathbf{r},\mathbf{r}_0)]^*\exp[-i2\pi\mathbf{k}\cdot\mathbf{r}]\mathrm{d}^2\mathbf{r}. \end{aligned} \tag{6}$$

Optics EXPRESS

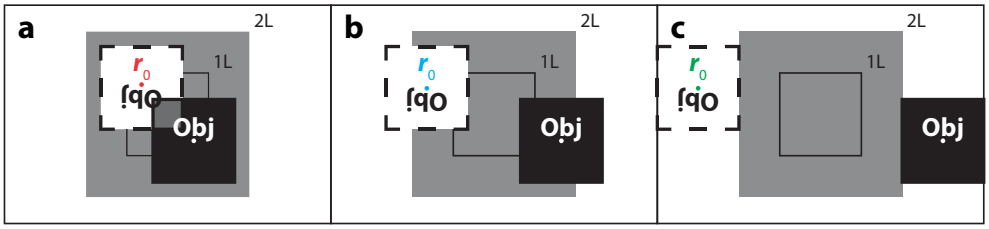

Fig. 2. The relations between the quadratic term (the original unperturbed diffraction pattern) and the two interference terms in the inverse Fourier transform of the perturbed diffraction pattern versus the location of the perturbation point $\mathbf{r}_0$. We use different colors to mark different values of $\mathbf{r}_0$. The gray square at the origin denotes the quadratic term which is twice as large as the aperture. The black square and the white square denote the transmission function and its complex-conjugate in the two interference terms respectively.

Eq. (6) shows that the introduction of the perturbation creates two interference terms which are directly proportional to the product of $T(\mathbf{r})$, the transmission function of the aperture plane, and $J(\mathbf{r}, \mathbf{r}_0)$, the correlation between the field at the perturbation point $\mathbf{r}_0$ and at all other points $\mathbf{r}$. One term in Eq. (6) is the inverse FT of the interference term containing $T(\mathbf{r})J(\mathbf{r}, \mathbf{r}_0)$ which is shifted to the mirrored location of the perturbation point at $-\mathbf{r}_0$ and the other term is the inverse FT of the interference term containing $[T(\mathbf{r}')J(\mathbf{r}', \mathbf{r}_0)]^*$ is shifted to the location of the perturbation point $\mathbf{r}_0$ and is rotated by 180 degrees ($\mathbf{r}' = -\mathbf{r}$), which is known as the twin image in holography.

We can consider that perturbing the transmission function of the aperture plane at a point is equivalent to generating a spherical wave centered at this location. After propagation to the far-field, the spherical wave becomes a plane wave whose incident angle on the detector is determined by the location of the perturbation point. The plane wave interferes with the partially coherent beam that propagates through the aperture and the object in the detector plane and results in two interference terms. Thus, moving the perturbation point will change the locations of the two interference terms, which is exactly the same as that in the coherent holography.

The correlation $J(\mathbf{r}, \mathbf{r}_0)$ now plays a role as a modulation of the transmission function of the aperture plane $T(\mathbf{r})$. For coherent illumination, this modulation is a constant. However, for partially coherent illumination, the modulation may have a certain distribution in both amplitude and phase according to the spatial coherence properties. In the limiting situation of incoherent illumination, this modulation is a delta function, and then we cannot retrieve any information from the two interference terms. We refer to $J(\mathbf{r}, \mathbf{r}_0)$ as a "slice" of the MCF because it describes a two-dimensional cross-section of the MCF in the 4-dimensional space. $J(\mathbf{r}, \mathbf{r}_0)$ depends on the spatial coherence properties of the illumination beam as well as the location where we introduce the perturbation point.

2.2. *Methods for retrieving the interference terms*

The key of our method is to extract the two interference terms from the intensity measurements. We illustrate the relation between the quadratic term, corresponding to the original diffraction pattern $I_0(\mathbf{k})$, and the two interference terms in the inverse FT of the intensity measurement $I(\mathbf{k})$ in Fig. 2. Here we neglect the constant term $|\gamma - 1|^2 J(\mathbf{r}_0, \mathbf{r}_0)$ because its inverse FT is a delta function. It is shown that the quadratic term is always centred at the origin, but the locations of the inverse FT of the two interference terms depend on the the location of the perturbation point $\mathbf{r}_0$. Moreover, because they are located symmetrically on both sides of the origin, by varying $\mathbf{r}_0$, we can change the separation distance between them and hence change the overlap between each other as well as the overlap between them and the quadratic term.

When we introduce the perturbation point inside the aperture as shown in Fig. 2(a), the

Optics EXPRESS

two interference terms overlap with the quadratic term and with each other. We need three measurements to retrieve both parts of these two interference terms [4, 27]. One of them is the original intensity measurement $I_0(\mathbf{k})$, which corresponds to the case of $\gamma = 0$, and the other two measurements, $I_C(\mathbf{k})$ and $I_D(\mathbf{k}$, correspond to two different perturbation values, γ_C and γ_D), at the same perturbation location. In this way, we can create a system of linear equations:

$$\begin{cases} \mathcal{F}^{-1}\{I_C(\mathbf{k}) - I_0(\mathbf{k})\} = C^*A + CB^* \\ \mathcal{F}^{-1}\{I_D(\mathbf{k}) - I_0(\mathbf{k})\} = D^*A + DB^* \end{cases}, \tag{7}$$

where

$$\begin{cases} A = T(\mathbf{r}_0 + \mathbf{r})J(\mathbf{r}_0 + \mathbf{r}, \mathbf{r}_0) \\ B = T(\mathbf{r}_0 - \mathbf{r})J(\mathbf{r}_0 - \mathbf{r}, \mathbf{r}_0) \end{cases}, \text{ and } \begin{cases} C = (\gamma_C - 1)T(\mathbf{r}_0) \\ D = (\gamma_D - 1)T(\mathbf{r}_0) \end{cases}, \tag{8}$$

From Eq. (7), we can solve for the two interference terms as follows:

$$\begin{cases} A = [D\ \mathcal{F}^{-1}\{I_C(\mathbf{k}) - I_0(\mathbf{k})\} - C\ \mathcal{F}^{-1}\{I_D(\mathbf{k}) - I_0(\mathbf{k})\}][C^*D - D^*C]^{-1} \\ B = [D^*\mathcal{F}^{-1}\{I_C(\mathbf{k}) - I_0(\mathbf{k})\} - C^*\mathcal{F}^{-1}\{I_D(\mathbf{k}) - I_0(\mathbf{k})\}][D^*C - C^*D]^{-1} \end{cases}. \tag{9}$$

When we introduce the perturbation point outside the aperture, the two interference terms are already separated from each other. If they overlap with the quadratic term as shown in Fig. 2(b), then in addition to the intensity measurement $I(\mathbf{k})$, we also need to measure the original intensity distribution $I_0(\mathbf{k})$ to eliminate the quadratic term [24]. Finally, if the two interference terms do not overlap with the quadratic term as shown in Fig. 2(c), we only need to measure $I(\mathbf{k})$ [21–23].

3. Experimental validation

The experimental setup is shown is Fig. (3). We focus a coherent laser beam onto a diffuser. The focused laser light will then be modulated by a random phase and generates a speckle pattern. As we rotate this diffuser, during the integration time of the camera, all the speckle patterns add incoherently. Therefore, we can reduce the degree of coherence of the focused laser light to zero and create an incoherent source provided that the rotation is fast enough or the integration time is long enough. Alternatively, we can consider that the scattered light at different locations in the area illuminated by the focused laser beam are independent of each other because the phase modulation varies randomly as time changes. Consequently, the incoherent source consists of a collection of independent point sources. Their sizes and the separation between them are determined the roughness of the diffuser.

The light emitted by this incoherent source is then collimated before illuminating the aperture and a phase object in the aperture plane (the plane where we reconstruct the MCF of the incident beam and the transmission function of the phase object). The intensity distribution of this incoherent source (the focal spot of the coherent laser beam) determines the spatial coherence properties of the illumination beam. In the experiment, we can obtain two different focal spot distributions and generate two differently correlated beams: the Gaussian correlated beam, also known as the Gaussian Schell-model (GSM) beam, and the Gaussian-Airy correlated beam. The difference is that the profile of the coherent laser beam is truncated by the focusing lens in the latter case but not in the former case. We vary the degree of coherence by changing the size of the focal spot, which is done by translating the focusing lens back and forth. In the case when the size of the focal spot is smaller than the diffraction limit of the collimation lens, the source generates coherent illumination. In other cases, it generates partially coherent illumination.

We place a reflective phase only spatial light modulator (SLM) in the aperture plane as shown in Fig. 3. It simulates the effect of the aperture and the phase object. The aperture is a square of 240×240 pixels on the SLM. The light inside the aperture, which is modulated by the

Optics EXPRESS

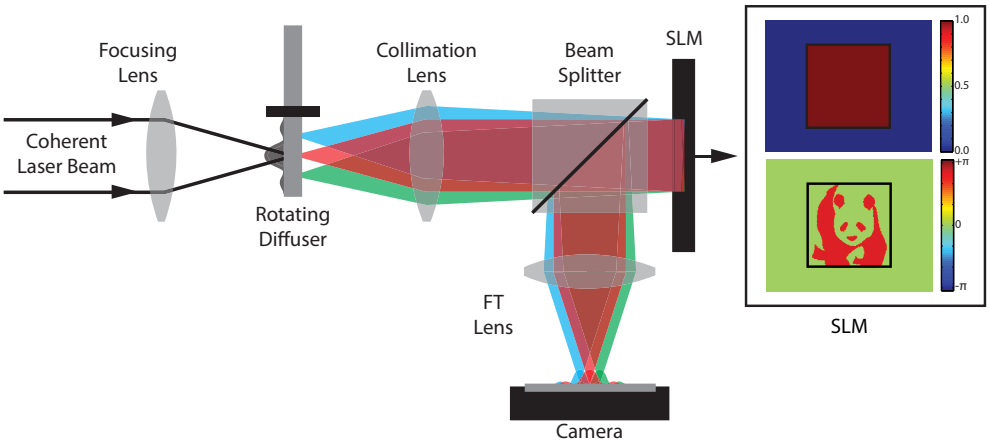

Fig. 3. The experimental setup. The partially coherent beam is generated by focusing coherent laser beam onto a rotating difusser. By varying the intensity distribution of the focal spot, we can change the spatial coherence properties of the generated beam. We then collimate the generated beam and use it to illuminate a SLM, on which we simulate the effect of the aperture as well as the phase object. Finally, we measure intensity distribution of the Fourier transform (FT) of the light field at the SLM using a FT lens.

transmission function of the phase object, is directly reflected to the direction of the detector, while the light outside the aperture is reflected to other directions by using phase tilt. The phase object has uniform amplitude and binary phase distribution between 0.1π and 0.9π in the shape of a panda. In the experiment, we introduce the perturbation point by varying the phase in a region of 10×10 pixels. When the perturbation point inside the aperture, we change the phase of the phase object in the region of perturbation by $\pm\pi/2$. When the perturbation point is outside the aperture, we switch the direction of the reflected light to mimic the effect of "open" (reflect towards the detector) and "close" (reflect towards other directions) a pinhole.

The far-field propagation from the SLM (the reconstruction plane) to the detector can be approximated by a Fourier transform. This can be achieved by Fresnel or Fraunhofer propagation in free space, e.g. in the X-ray and electron regime, or by using a Fourier transform lens for visible wavelength as we did in the experiment. The reconstruction plane and the detector should be at the front and back focal planes of the Fourier transform lens respectively.

3.1. Results of varying the location of the perturbation point for GSM beam illumination

It is shown in Eq. (6) that by varying the location of the perturbation point $\mathbf{r}_0$, we can change the separation between the two interference terms. This phenomenon is demonstrated experimentally in Fig. 4. In the experiment, we illuminate a phase object using a GSM beam. Because the MCF of the GSM has a uniform phase, the phases of the inverse FT of the two interference terms are the same as the phase of the object $O(\mathbf{r})$. Moreover, the amplitudes of the inverse FT of the two interference terms are the same as the amplitude of the slice of the MCF of the GSM $J(\mathbf{r}, \mathbf{r}_0)$. Note that the panda shape in the amplitude is due to the phase discontinuity.

We can see in the figure that the further we move the perturbation point from the origin, the more the two interference terms become separated from each other. This obviously changes the amount of overlap between different terms since the quadratic term will always be centred at the origin. Consequently, the further the perturbation point is located from the origin, the less the inverse FT of the two interference terms overlap with each other and with the quadratic term.

When the perturbation point is located inside the aperture as shown in Fig. 4(a1) and 4(a2),

Optics EXPRESS

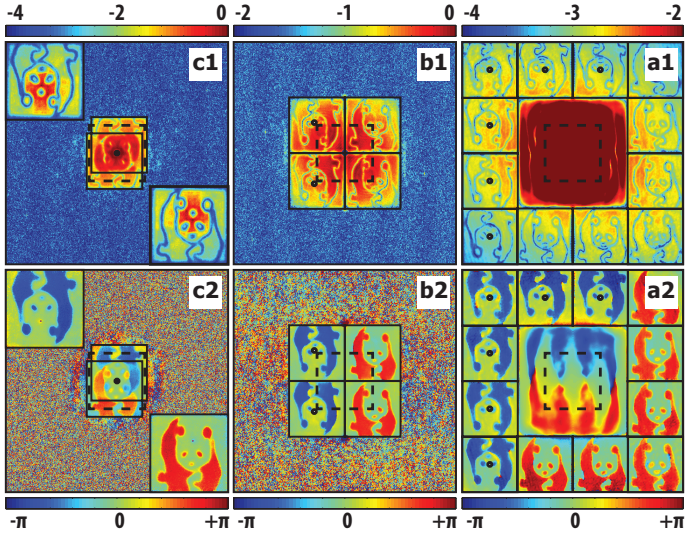

Fig. 4. Experimental results for varying the location of the perturbation point for a GSM beam. (a,b,c): results for three different overlapping conditions, which require different number of measurements to retrieve the two interference terms. The squares in the figure are the products of the correlation function $J(\mathbf{r}, \mathbf{r}_0)$ and the aperture plane's transmission function $O(\mathbf{r})$. The red panda and the blue panda represent the trasmission function and its complex-conjugate in the two interference terms respectively.

only one perturbation point can be introduced, because otherwise, the interference terms created by different perturbation points will overlap and cause problems in the retrieval. When the perturbation point is located outside the aperture, there is room for introducing more than one perturbation point simultaneously, as long as there is no overlap between the interference terms created by different perturbation points. In Fig. 4(b1) and 4(b2), we introduced two perturbation points, and the generated interference terms fill the area occupied by the quadratic term. In Fig. 4(c1) and 4(,c2), we introduced six perturbation points which generate interference terms filling the area around the quadratic term.

Figure 4 illustrates that as we vary the location of the perturbation point $\mathbf{r}_0$, we also change the slice of the MCF $J(\mathbf{r}, \mathbf{r}_0)$ we measure. Note that we can only measure the part that falls on the area defined by the size of the aperture. Eq. (6) indicates that the correlation is maximal when the two coordinates of the MCF coincide ($\mathbf{r}_0 \pm \mathbf{r} = \mathbf{r}_0$), so the peak of the correlation function will always appear at the origin ($\mathbf{r} = 0$). We observe in the figure that as we move $\mathbf{r}_0$ further from the origin, the area of measurement shifts further too. For GSM beam whose MCF is shift-invariant, we then measure different part of the same Gaussian profile.

3.2. *Results of varying the degree of coherence of the GSM beam*

In Fig. 5 we compare the experimental results using a GSM illumination beam for two different degrees of coherence. Since the amplitudes are the same as the amplitude of the slice of the MCF of the GSM beam, we can fit it by a Gaussian distribution: $z = \exp[-|\mathbf{r}|^2/(2\sigma^2)]$ where σ is the width of the Gaussian distribution linked to the degree of coherence of the illumination in the aperture plane. In Fig. 5(a2) and 5(b2), the fitting results demonstrate that the amplitude indeed follows the Gaussian distribution. Moreover, in Fig. 5(a3) and 5(b3), the results show that the degree of coherence influences the field-of-view by modulating the amplitude

Optics EXPRESS

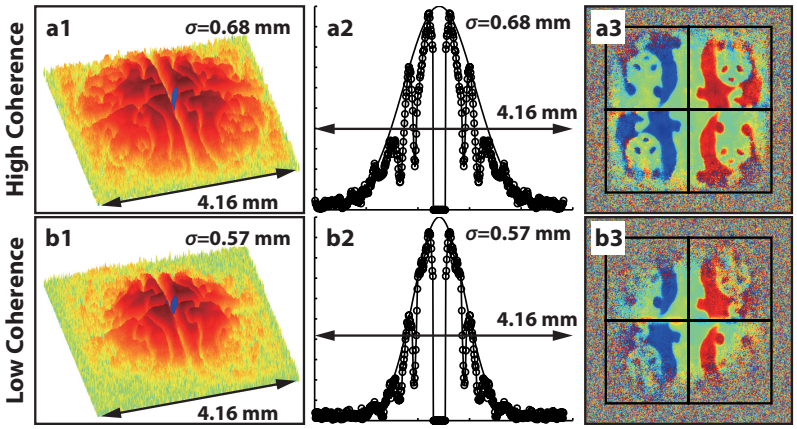

Fig. 5. Experimental results of varying the degree of coherence of the GSM beam. The locations of the perturbation points are chosen such that we can observe the whole Gaussian profile. (a1), (b1): amplitudes of the two interference terms. (a2), (b2): results of fitting to the amplitude's cross-section. (a3), (b3): the phase of the two interference terms.

We can only retrieve the amplitude and the phase of the two interference terms in the area where the amplitude of the illuminating beam is substantially higher than the noise. The size of this area is determined by the noise level and the degree of coherence of the illumination. For illumination using s GSM beam, the transmission function of the object is modulated by a Gaussian distribution. Since this modulation decreases as the distance to the perturbation point increases, the transmission function $T(\mathbf{r})$ further from the origin is more influenced by noise. When the illumination is perfectly spatial coherent, the modulation is constant, whereas if the illumination is completely spatially incoherent, the modulation is a delta function at the origin. Using a partially coherent illumination gives results between these two extreme cases. It is shown in Fig. 5(a3) and 5(b3) that the resolution is independent of the change of the degree of coherence. It also stays the same at different locations of the illuminated area.

3.3. *Results of varying the degree of coherence of the Gaussian-Airy correlated beam*

In the previous example, we have seen that the MCF of the GSM beam has a uniform flat phase. However, in more general cases, e.g. the Gaussian-Airy correlated beam, the MCF may have a more complicated phase distribution. Since this phase distribution will affect the results of diffractive imaging and other applications, it is necessary to measure not only the amplitude but also the phase of the MCF.

In Fig. 6 we found that the amplitudes of the inverse FT of the two interference terms are still the same as the amplitude of the MCF of the Gaussian-Airy beam that illuminates the phase object, but the phases is a product of the phase of the MCF of the illumination beam and the phase of the object. The amplitude of the MCF of the Gaussian-Airy correlated beam consists of a number of rings, and the number of rings depends on the degree of coherence of the beam. The phase of the MCF jumps between 0 and π at the locations where the amplitude vanishes. This suggests that the correlation between the fields at these locations and at the location of the perturbation point changes sign. The phase of the retrieved transmission function of the object is obscured by the phase of the MCF, although the panda is still clearly visible.

The obscuration of the object by the slice of the MCF of the illumination beam can be regarded as a modulation. In order to retrieve the pure object, we need to calibrate and then compensate for this modulation. For the calibration, we place the perturbation points at exactly the same

Optics EXPRESS

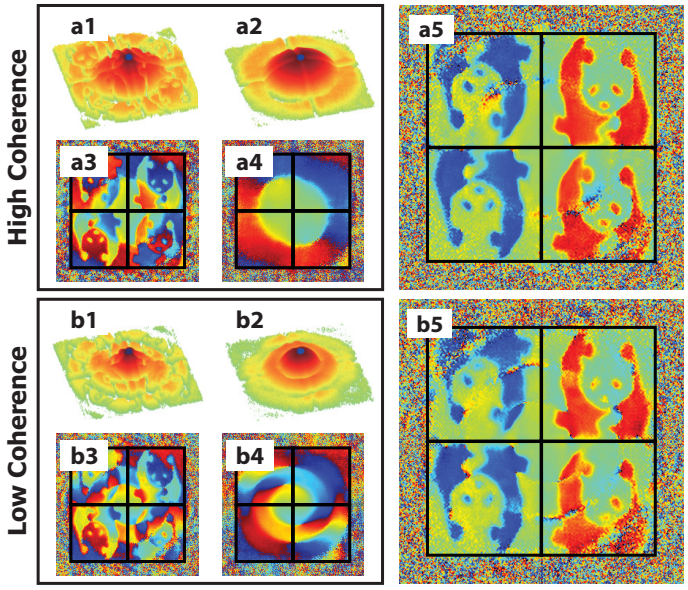

Fig. 6. Experimental results of varying degree of coherence of the Gaussian-Airy correlation beam. (a1,b1 and a3,b3): the amplitude and the phase of the two interference terms in the presence of the phase object. (a2,b2 and a4,b4): the amplitude and the phase of the two interference terms in the absence of the phase object. (a5,b5): the phase of the results after modulation compensation.

locations, the two left corners of the aperture, to guarantee that we measure the same slices of the MCF of the illumination beam. We then divide the obscured transmission function of the object by the calibration results of the illumination beam. This yields an almost perfect reconstruction of the object as shown in Fig. 6(a5) and 6(b5).

4. Discussion and conclusion

In this paper, we have demonstrated that using our non-iterative method, the 4-dimensional MCF of an arbitrary spatially partially coherent beam can be accurately determined. Our method measures the MCF slice by slice; each slice being a 2-dimensional complex-valued correlation function between the perturbation point and all other points retrieved from diffracted far-field intensities. The procedure of retrieval is similar to holography. An essential feature of our method is that the reference is created by perturbing the transmission function of the aperture plane at one or more locations. This creates a coherent reference as if emitted by a point source in the aperture plane, and more importantly, it is correlated with the partially coherent field that propagates through the aperture and the object. In contrast, in holography, a beam splitter is used in the light path, so that the reference is also spatially partially coherent and therefore, it is impossible to retrieve the MCF of the incident beam or reconstruct the transmission function from the interference pattern. Our method also shows that FT holography [21–23] and Zernike phase-shifting holography [27] are in principle able to deal with spatial partially coherence effect.

Traditionally, it was believed that interferometry, holography and iterative diffractive imaging techniques all require coherent illumination to retrieve a complex-valued transmission function of the object because the randomly fast varying phase of the partially coherent fields was expected to destroy the phase information carried by the intensity measurements. The smaller the degree of coherence of the illumination, the more difficult the retrieval of the phase of the transmission

Optics EXPRESS

function would be. However, as we have demonstrated, this is not necessarily the case. We found that when the degree of coherence is smaller, only the area over which the object can be reconstructed becomes smaller. The experimental results confirm that the use of partially coherent illumination only leads to a modulation of the object. We demonstrated that the reconstruction of the object depends on the signal-to-noise ratio of the intensity measurements, which is determined by the amplitude of the MCF of the illumination beam and the noise level. By correcting for this modulation, the object can be reconstructed as if coherent illumination was used.

The resolution of the retrieved MCF, as well as the reconstructed object, is determined by the size of the perturbation region. However, we cannot make this region very small because then the energy of the two interference terms will be too small to be detected. In contrast, the energy of the quadratic term, which is given by the intensity of the light propagating through the aperture, is very large. To balance the energies of the two interference terms and of the quadratic term, one can either focus a part of the illumination beam to the location of the perturbation point to boost the intensity of light there, or reduce the intensity of light propagating through the aperture.

The signal-to-noise ratio of the intensity measurements is basically limited by the dynamic range of the detector. Most of the objects generate a diffraction pattern with a strong peak and weak side lobes. Due to the limited number of grey levels of the detector, the diffraction pattern cannot be resolved properly. This problem can be solved by using a diffuser to modulate the wavefront of the incident illumination beam. Because the phase of the diffuser varies rapidly at different locations, the generated diffraction pattern will then be more spread and thus have smaller difference between the peak and the side lobes. This has already been tested and proved to be useful for coherent ptychography in [28], and we will implement it in our future work.

In this paper, we restrict our discussion to only quasi-monochromatic light. If the spatially partially coherent beam is chromatic, we then need to take into account scaling effect of free-space propagation. In the Fraunhofer or the Fresnel approximation, the size of the intensity distribution at the detector plane is in proportional to the reciprocal wavelength. Since only part of the scaled intensity distribution falls on the detector, the size of this part varies for different wavelengths, which then leads to the variation of the resolution of the result after inverse Fourier transform. Therefore, using chromatic illumination, the result will be a superposition of the MCFs with different resolutions. For Fourier transform using lenses, the dispersion of the lenses may bring chromatic aberrations to the intensity measurements, for example, the lens will have different focal length for different wavelengths causing blurry of the intensity measurements, and this situation then will be too complicated to analyse.

To conclude, our method is among the most efficient methods for spatial coherence measurement, and is robust against noise. Besides, it retrieves both the amplitude and the phase from the far-field intensities. This feature makes it a competitive approach for a broad range of applications, since from the knowledge of the complete MCF in the measurement plane, one can calculate the MCF and the associated intensity distribution in any other planes. In the experiment, we use a SLM to introduce the perturbation to the transmission of the measurement plane, but in certain wavelength range, e.g. the X-ray and the electron regime, we cannot find a device analogous to a SLM. It has been reported that diffractive imaging can be achieved by using pinhole as perturbation [21–23]. We believe this research can also help extending diffractive imaging to use spatially partially coherent illumination.

Funding

Netherlands Organisation for Scientific Research (NWO) (“Novel design shapes for complex optical systems” (12798)); National Natural Science Foundation of China (11774250, 91750201 and 1374222); National Natural Science Fund for Distinguished Young Scholars (11525418); Qing Lan Project of Jiangsu Province; Jiangsu Overseas Research & Training program for University Prominent Young & Middle-aged Teachers and Presidents.